

Research on the Mechanism of Exosomes Derived from Bone Marrow Mesenchymal Stem Cells Delivering circ-Snhg11 to Promote Diabetic Wound Healing

Jingyu Qian^{1, a}, Longji Ye^{2, b}, Xiaoyun Tang^{1, c}, Panpan Jin^{2, d}, Junfeng Shao^{2, *}

¹ Department of Interventional Radiology, The First Affiliated Hospital of Bengbu Medical University, Bengbu, Anhui 233000, China

² Department of General Medicine, The First Affiliated Hospital of Bengbu Medical University, Bengbu, Anhui 233000, China

* **Corresponding author:** Junfeng Shao (Email: sjf_bbmc@163.com), ^a jyqian1388@163.com, ^b yljjy@163.com,

^c 18255028962@163.com, ^d 17855786369@163.com

Co-first authors: Jingyu Qian and Longji Ye contributed equally as co-first authors

Abstract: Background: The ability of BMSC-derived exosomes (BMSC-Exos) to accelerate diabetic wound healing has been observed, but the underlying mechanism has not been fully elucidated. Methods: Differential expression of circRNA in skin tissue before and after exosome treatment was analyzed using second-generation sequencing technology. The targeting relationship between circRNA and downstream targets was detected using a luciferase reporter gene assay. Results: Exosome treatment significantly promoted diabetic wound healing. NGS results indicated that circ-Snhg11 was involved in exosome-mediated tissue repair. Knockdown of circ-Snhg11 attenuated the effect of exosomes on accelerating diabetic wound healing. Luciferase reporter gene data confirmed the targeting interaction between circ-Snhg11, SLC7A11, and miR-144-3p. Conclusion: BMSC-Exos promote diabetic wound healing by delivering circ-Snhg11, which is related to the regulation of endothelial cell ferroptosis mediated by SLC7A11/GPX4.

Keywords: circ-Snhg11; Exosomes; Diabetic Wound Healing; Ferroptosis; SLC7A11; miR-144-3p.

1. Introduction

Vascular damage caused by hyperglycemia may be a major reason for severe symptoms such as diabetic ulcers[1,2]. Therefore, research into new therapeutic approaches for diabetic ulcers is crucial.

Inflammation and ferroptosis induced by the diabetic hyperglycemic microenvironment are important reasons for difficult wound healing[3]. Excessive expression of inflammatory factors can impair angiogenesis [4,5]. Autologous stem cell transplantation is used in regenerative plastic surgery[6] and to prevent skin photoaging caused by ultraviolet (UV) radiation[7]. An increasing number of studies have confirmed that exosomes (Exos) derived from mesenchymal stem cells play an indispensable role in regulating angiogenesis-based wound healing[8,9,10,11]. Exosomes are double-layered vesicle bodies with a diameter of 40-50 nanometers, originating from the endosomal system, facilitating intercellular communication by delivering miRNAs, circular RNAs (circRNAs), and mRNAs.[12]. CircRNAs also regulate gene expression, which makes them potential biomarkers for diagnostic and therapeutic applications.[13].

We will explore the potential mechanism of Exos produced by BMSCs in diabetic wound healing and identify downstream regulatory genes, aiming to provide new perspectives for cell therapy in regulating diabetic wound healing.

2. Methods

2.1. Isolation, Identification, and Cultivation of Mesenchymal Stem Cells from Bone Marrow

Femurs and tibias of BALB/c mice were collected, and the bone marrow filtrate was separated by centrifugation at 225×g. The sample was mixed with an equal volume of mouse lymphocyte separation medium, centrifuged at 1000×g, and then resuspended in low-glucose (LG)-DMEM. The pellet was reconstituted in LG-DMEM with FBS and cultured in a humidified 5% CO₂ incubator. Upon reaching 80–90% confluence, cells were passaged at a 1:3 ratio. BMSCs at passages III or IV were used for downstream assays. For phenotyping, phycoerythrin (PE)-conjugated antibodies targeting CD105, CD29, CD44, CD90, and vWF were employed.

2.2. Multilineage Differentiation Potential of BMSCs

After two weeks, osteogenic differentiation was observed using ALP or alizarin red staining.

2.3. Isolation of BMSC-Exo

When the fusion degree of BMSCs reaches 80-90%, wash them with PBS and then culture them in EGM-2MV medium supplemented with 1-fold serum substitute without FBS. Collect the culture medium, centrifuge at 2000×g to remove apoptotic cells and debris, and then centrifuge at 12,000×g for 0.5 hours at 4°C. BMSC-Exos are stored at -80°C or used immediately for subsequent experiments. Characterize the extracted exosomes by Western blotting and NTA.

2.4. Library Preparation for Strand-Specific NGS

Skin tissue samples were collected from DM mice either receiving or not receiving Exos treatment (48 hours after exosome injection). For Illumina sequencing, ribosomal RNA was depleted from roughly 3 µg of total RNA. The purified RNA was then digested with 40 U of RNase R at 37°C, and RNA-seq libraries were constructed.

2.5. Cell Culture and Transfection

Endothelial progenitor cells were purchased. Overexpression vectors for SLC7A11 and circ-Snhg11 were generated using the pcDNA3.1 vector. Transfection was performed using Lipofectamine 2000, and cells were cultured in high-glucose DMEM (30 mM glucose).

2.6. RT-PCR and RNA Isolation

PCR was performed using 2×Taq PCR Master. Fold changes were quantified using the $2^{-\Delta\Delta Ct}$ method. The PCR primers used were as follows:

circ-Snhg11: Forward 5'-GTTCTGTGTGGTTCCTC-3', Reverse 5'-CGCCGGGTCCC-3'; SLC7A11: Forward 5'-TCGCTGGTGTGGTTTG-3', Reverse 5'-CTTCTCCCTTCCGC-3'; GPX4: Forward 5'-ATACGGGGGGGGT TGGTTTGGGC-3', Reverse 5'-CTTCATCCCCCACCA GCG-3'; GAPDH: Forward 5'-GGGGGGGGGGGGGGG AAG-3', Reverse 5'-TAGGGGGGGGGTTTGAAC-3'.

2.7. Dual-Luciferase Reporter Assay

The circ-Snhg11/SLC7A11 3'UTR containing the miR-144-3p binding site was amplified and inserted into a luciferase reporter vector. 0.1 µg of the luciferase reporter vector was co-transfected with EPC, and similar procedures were performed for miR-control.

2.8. ROS Analysis

In brief, EPCs were seeded in culture dish, stained with DAPI, and then exposed to DCF-DA for 10 minutes. Subsequently, cells were subjected to normoxic or hypoxic

treatment, and ROS levels were assessed by measuring the fluorescence intensity of DCF-DA.

2.9. Tube Formation Assay

The research team evaluated the in vitro angiogenesis ability of serum-starved EPCs under 37°C culture conditions. In brief, capillary-like networks embedded in Matrigel were visualized by phase contrast microscopy. The length of tube-like structures was measured in 10 randomly selected fields.

2.10. Diabetic Wound Induction

To generate diabetic models, male BALB/c mice were given a single intraperitoneal STZ injection (60 mg/kg). Following a one-month stabilization period, individuals with fasting glucose levels >250 mg/dL were deemed diabetic and enrolled in the study. First, the dorsal hair on the legs was disinfected with povidone-iodine, and then a 4-mm full-thickness skin excision wound was made. Animals were randomly assigned and received subcutaneous injections at four wound-margin sites with 200 µg of BMSC-Exos or an equal volume of PBS. Mice were euthanized 15 days later, and skin samples were cultured, with 6 mice per group.

2.11. Immunohistochemistry

Tissue sections embedded in paraffin were incubated overnight with primary antibodies targeting GPX4 or CD31 overnight, and then stain them with 3,3-diaminobenzidine.

2.12. Statistical Analysis

Statistical analysis was performed using GraphPad Prism. A threshold of $P < 0.05$ was regarded as statistically significant. Differences between two groups were calculated using two-tailed Student's t-test. For comparisons among three or more groups, one-way and two-way ANOVA were applied to assess significant differences.

3. Results

Characterization of BMSCs and Exos

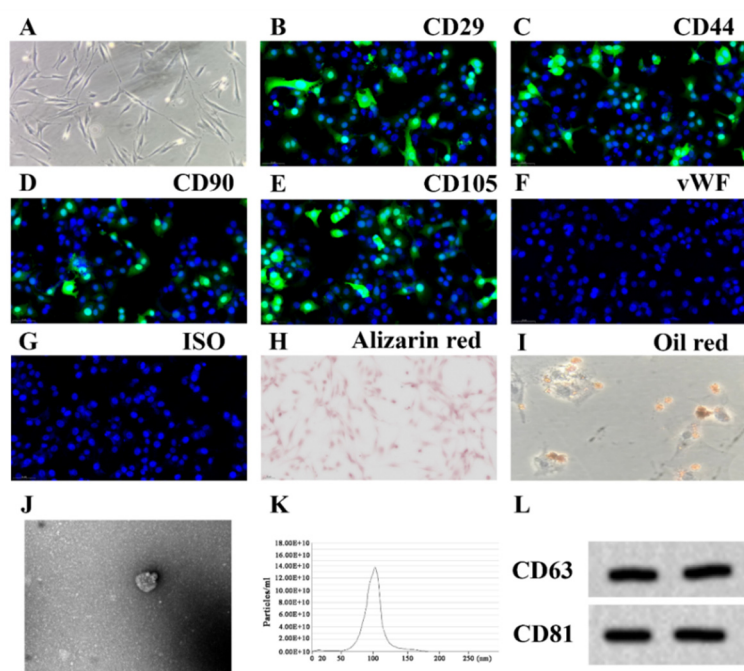


Figure 1. Properties of BMSC-Exos Isolated from Culture Medium

Note:(A) BMSCs showed a classic cobblestone-like appearance. (B-G) Surface markers were identified by immunofluorescence staining. PE-labeled antibodies appeared red. Cells were positive for CD90, CD105, CD44, and CD29, but negative for vWF. (H-I) Multilineage differentiation capacity of BMSCs was assessed using alkaline phosphatase (H) and oil red O (I) staining. (J) Transmission electron microscopy revealed the morphology of BMSC-Exos. (K) NanoSight analysis determined the size distribution of purified BMSC-Exos. (L) Western blotting confirmed CD43 and CD81 expression in BMSC-Exos.

In this study, BMSCs with a typical fibroblast-like spindle shape were extracted, as shown in Figure 1A. Immunofluorescence staining confirmed that the isolated cells expressed CD29 (#ab179471, 1:500, abcam, USA), CD105 (#ab221675, 1:500, abcam, USA), CD44 (#ab243894, 1:500, abcam, USA), and CD90 (#ab307736, 1:500, abcam, USA), while negative for the endothelial marker vWF (#ab287962, 1:500, abcam, USA) (Figure 1B-G). The adipogenic and osteogenic differentiation capacities of BMSCs were verified

by through Oil Red O and ALP staining, respectively (Figure 1h-1). Transmission electron microscopy confirmed that BMSC-Exos exhibited a spherical or cup-shaped morphology (Figure 1J), consistent with previous research findings[14]. NTA results showed that the average diameter of Exos was approximately 100 nm (Figure 1K). Western blot analysis was used to detect the expression of Exo marker proteins, including CD81 (#ab109201, 1:500, abcam, USA) and CD63 (#ab217345, 1:500, abcam, USA) (Figure 1L).

3.1. Effect of BMSCs-Exos on Wound Healing

BMSC-Exo promoted diabetic wound healing (Figure 2A-B). Exos treatment inhibited ROS deposition (Figure 2C-D). Furthermore, GPX4 immunofluorescence staining showed that Exos treatment promoted GPX4 expression (Figure 2C-D), indicating that Exos administration alleviated HG-induced ferroptosis. Exos treatment enhanced CD31 expression at the ulcer site, as revealed by immunofluorescence (Figure 2E-F).

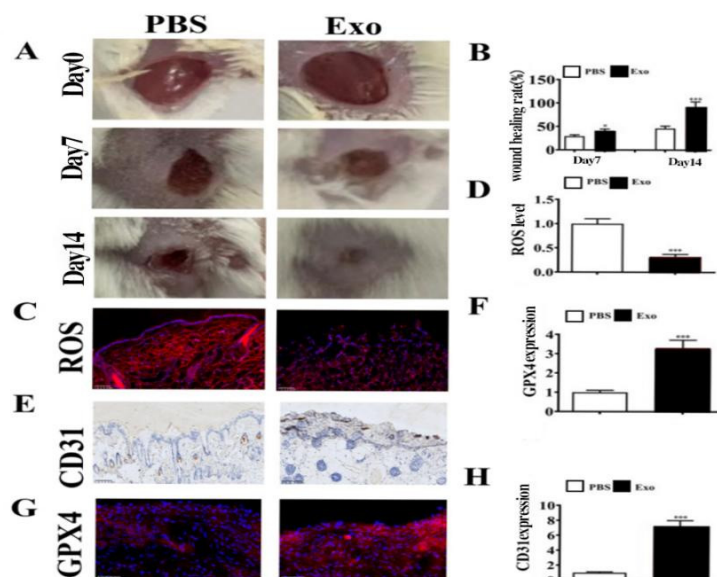


Figure 2. Effect of BMS-Exo treatment on wound healing

Note: Effect of BMS-Exo on wound healing. (A-B) Representative wound images and healing rate quantification (n=6). (C-D) ROS levels. (E-F) GPX expression. (G-H) CD31 expression. Data are mean ± SD. *p<0.05, ***p<0.001 vs. PBS group.

3.2. Function of circ-Snhg11 in Wound Healing Mediated by BMSC-Exos

NGS analysis revealed abnormal circRNA expression in diabetic mice following Exos treatment (Figure 3A). Specifically, RT-qPCR analysis showed that the expression of circ-Snhg11 was upregulated in the Exos group compared to the PBS-only group, as shown in Figure 3B. However, RT-qPCR showed decreased expression levels of circ-Snhg11 in serum (Figure 3C). Silencing circ-Snhg11 expression inhibited the protective effect of Exos (Figure 3D-E). Additionally, immunofluorescence analysis revealed that circ-Snhg11 knockdown normalized ROS levels (Figure 3F-G). Furthermore, GPX4 immunofluorescence staining demonstrated that circ-Snhg11 knockdown abolished the

enhancing effect of Exos treatment on GPX4 expression (Figure 3H). Similarly, CD31 immunofluorescence staining confirmed that circ-Snhg11 silencing reversed the promoting effect of Exos treatment on angiogenesis at the ulcer site, as shown in Figure 3K.

3.3. SLC7A11 is Crucial for BMSC-Exo-Mediated Wound Healing

NGS results showed abnormal mRNA expression in diabetic mice following Exos treatment (Figure 4A). RT-qPCR confirmed upregulation of SLC7A11 following Exo treatment relative to the PBS alone group (Figure 4B). RT-qPCR further indicated lower SLC7A11 levels in the serum of diabetic mice (Figure 4C). Knockdown of circ-Snhg11 led to reduced expression of SLC7A11, thereby accelerating diabetic wound healing (Figure 4D).

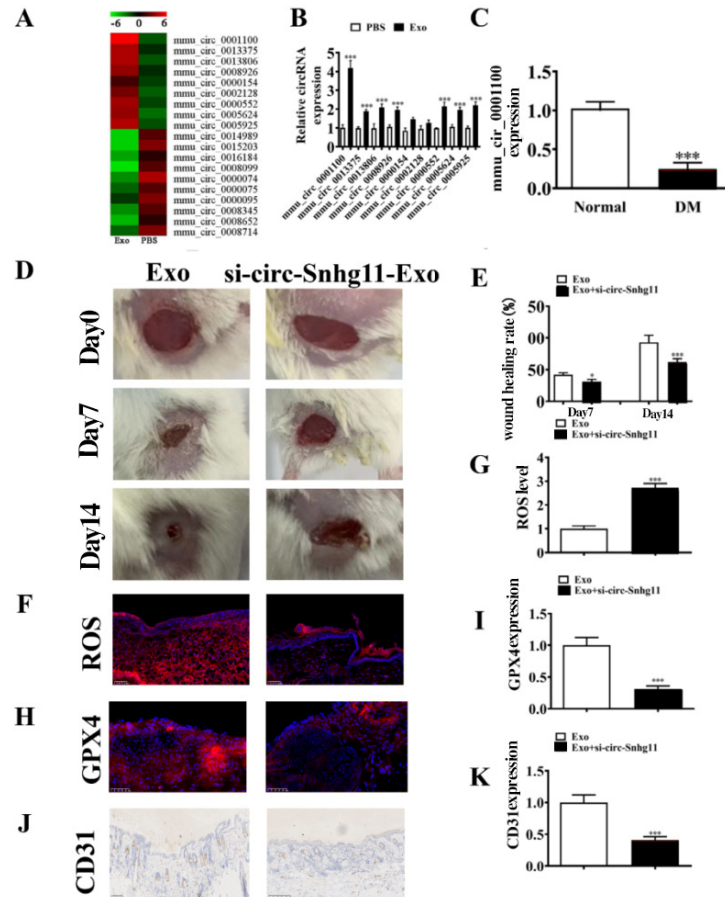


Figure 3. mmu_circ_000100 (circ-Snhg11) exerts an essential function in wound repair mediated by BMSC-Exo

Note: (A) NGS revealed differentially expressed circRNAs at the ulcer site (Exo vs. PBS). (B) RT-qPCR confirmed circRNA upregulation under Exo treatment. (C) RT-qPCR showed differential mmu_circ_000100 expression in serum (normal vs. diabetic mice). (D-E) Representative wound images and healing rate quantification (n=6). (F-G) ROS levels at the ulcer site by immunofluorescence. (H-I) GPX4 expression by immunofluorescence. (J-K) CD31 expression by immunohistochemistry. Data are mean \pm SD. * $P < 0.05$, *** $P < 0.001$ vs. Exo group.

3.4. SLC7A11 is a Downstream Target of circ-Snhg11

Bioinformatics analysis confirmed that mmu_circ_0001100 originates from the exon of Snhg11. Snhg11 and the spliced mature circRNA are both 660 bp long. Mmu_circ_0001100 was renamed circ-Snhg11. Specifically, miR-144-3p levels declined following Exos treatment (Figure 5B).

Luciferase reporter assays confirmed circ-Snhg11 directly regulates miR-144-3p (Figure 5C-D). To examine how SLC7A11 and miR-144-3p interact, we cloned the MUT or WT 3'UTR of SLC7A11 into a luciferase reporter plasmid (Figure 5E). These constructs were introduced into miR-144-3p mimic-treated and untreated EPCs. miR-144-3p reduced luciferase activity in wild-type cells (Figure 5F).

4. Discussion

BMSC-Exos exert their potential therapeutic effects through their protein and miRNA cargo during angiogenesis

[15]. Previous studies have shown that FHE hydrogels based on self-healing and antimicrobial peptides can repair chronic wounds by controlling the release of Exos as a multifunctional hydrogel [16,10,11]. The results of this study indicate that BMSC-Exo pretreatment improves diabetic wound repair. In particular, Exos treatment promoted angiogenesis and reduced ROS levels. Additionally, the expression of GPX4 was elevated following Exos treatment.

More studies have described the indispensable role of circRNAs in regulating biological processes [17,18]. Previous studies have confirmed that BMSC-Exos promote the growth and movement of human corneal epithelial cells in vitro by stimulating the p44/42 MAPK pathway, and inhibit alkali burn-induced corneal tissue inflammation, fibrosis, and angiogenesis in vivo [19]. Findings demonstrated that BMSC-derived exosomes or BMSC-Exos enhanced the growth and motility of HaCaT cells injured via the HO2 via miR-93-3p/APAF1 axis and inhibited apoptosis [20]. This study showed that Exos treatment upregulated circ-Snhg11, while circ-Snhg11 knockdown impaired Exos-mediated wound repair via suppression of angiogenesis and elevation of ROS levels, indicating that alleviating cellular stress and promoting vascularization accelerate wound healing.

Data from this study further show that Exos treatment resulted in elevated SLC7A11 expression. Ferroptosis inhibition restores vascular epithelial cell function [21,22]. Therefore, the study results suggest that Exos treatment enhances SLC7A11 expression, resulting in ferroptosis suppression and EPC functional recovery, thereby enhancing angiogenesis and wound repair. However, there are several limitations in this research. The expression of circ-Snhg11 in

clinical patients requires further investigation. We will also

determine the effects of circ-Snhg11 on cells other than EPCs.

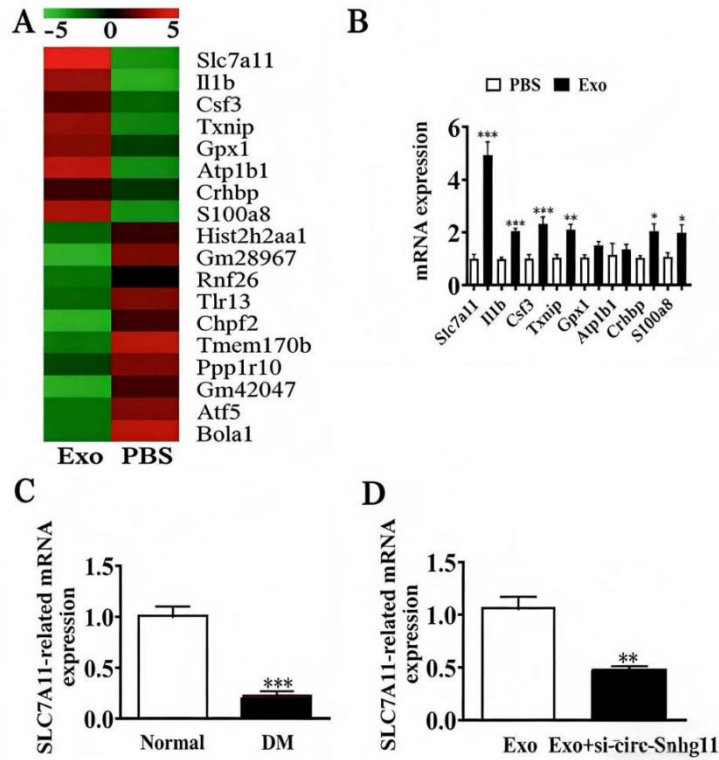


Figure 4. SLC7A11 Is Indispensable for BMSC-Exo-Promoted Wound Healing

Note: (A) NGS detected multiple differentially expressed mRNAs between the Exo and PBS treatment groups; (B) RT-qPCR confirmed that mRNA levels were elevated in the Exo group relative to the PBS group; (C) RT-qPCR compared the

expression levels of SLC7A11 in serum from normal versus diabetic mice; (D) RT-qPCR demonstrating SLC7A11 expression. Data are presented as mean \pm SD. *P < 0.05, **P < 0.01, ***P < 0.001 compared with Exo group.

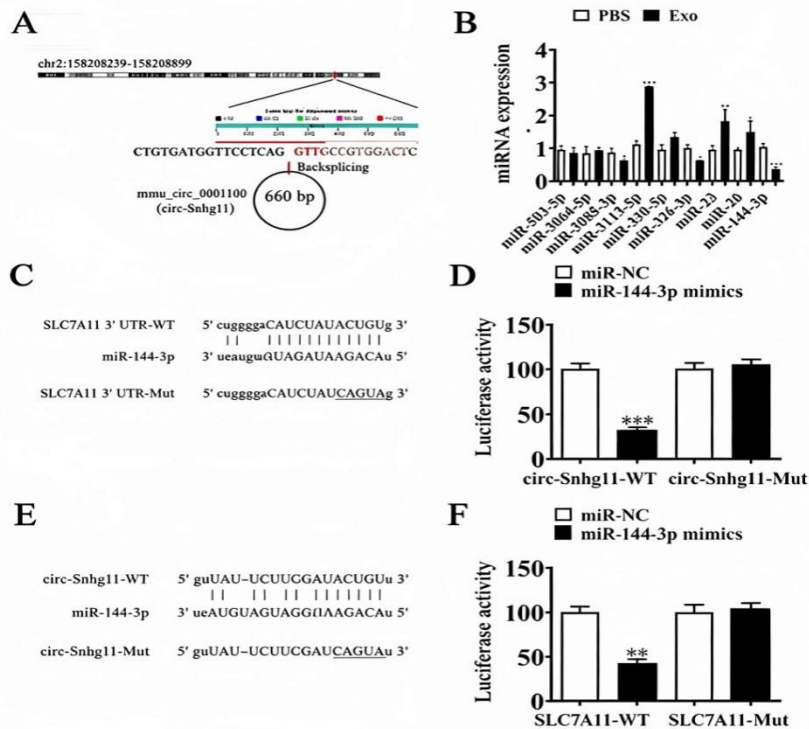


Figure 5. circ-Snhg11 targets SLC7A11 and miR-144-3p.

Note: (A) Genomic loci of Snhg11 and mmu circ 0001100. (B) RT-qPCR of miRNA-miRNA interactions. (C) Predicted miR-144-3p binding sites on circ-Snhg11 (WT and MUT). (D) Luciferase activity in HeK293T cells transfected with miR-

144-3p mimic/NC or circ-Snhg11 WT/Mut (48 h). (E) Predicted miR-144-3p binding sites in SLC7A11 3'UTR (WT and MUT). (F) Luciferase activity after transfection with miR-144-3p mimic/NC or 3'UTR-WT/Mut (48 h). Data are

mean \pm SD. * $P < 0.05$, ** $P < 0.01$, *** $P < 0.001$ vs. PBS.

5. Conclusion

The present results indicate that Exos derived from BMSCs accumulate in diabetic wound repair. Specifically, Exos in BMSCs promote diabetic wound repair through circ-Snhg11 delivery, in which the SLC7A11/GPX4-mediated anti-ferroptosis signaling plays a crucial role. Our research results provide new perspectives for cell-free therapy for diabetic wounds.

Acknowledgments

This work was supported by the Health Research Key Project of Anhui Province (Grant No. AHWJ2023BAc10022, 2023–2026) and the Natural Science Research Key Project of Anhui Universities (Grant No. KJ2021A0804, 2021–2023).

References

- [1] Yang J, Chen Z, Pan D, Li H, et al. Umbilical cord-derived mesenchymal stem cell-derived exosomes combined Pluronic F127 hydrogel promote chronic diabetic wound healing and complete skin regeneration. *Int J Nanomedicine*. 2020,15: 5911-26.
- [2] Everett E, Mathioudakis N. Update on management of diabetic foot ulcers. *Ann N Y Acad Sci*. 2018,1411(1):153-65.
- [3] Li S, Li Y, Wu Z, et al. Diabetic ferroptosis plays an important role in triggering inflammation in diabetic wound. *Am J Physiol Endocrinol Metab*. 2021,321(4):E509-20.
- [4] Liu W, Yu M, Xie D, et al. Melatonin-stimulated MSC-derived exosomes improve diabetic wound healing through regulating macrophage M1 and M2 polarization by targeting the PTEN/AKT pathway. *Stem Cell Res Ther*. 2020,11(1):259.
- [5] Kasuya A, Tokura Y. Attempts to accelerate wound healing. *J Dermatol Sci*. 2014,76(3):169-72.
- [6] Gentile P, Sterodimas A, Pizzicannella J, et al. Systematic review: allogenic use of stromal vascular fraction (SVF) and decellularized extracellular matrices (ECM) as advanced therapy medicinal products (ATMP) in tissue regeneration. *Int J Mol Sci*. 2020,21(14):4982.
- [7] Gentile P, Garcovich S. Adipose-derived mesenchymal stem cells (AD-MSCs) against ultraviolet (UV) radiation effects and the skin photoaging. *Biomedicines*. 2021,9(5):532.
- [8] Wang M, Wang C, Chen M, et al. Efficient angiogenesis-based diabetic wound healing/skin reconstruction through bioactive antibacterial adhesive ultraviolet shielding nanodressing with exosome release. *ACS Nano*. 2019,13(9):10279-93.
- [9] Yu M, Liu W, Li J, et al. Exosomes derived from atorvastatin-pretreated MSC accelerate diabetic wound repair by enhancing angiogenesis via AKT/eNOS pathway. *Stem Cell Res Ther*. 2020,11(1):350.
- [10] Li S, Li Y, Zhu K, He W, Guo X, Wang T, Gong S, Zhu Z. Exosomes from mesenchymal stem cells: Potential applications in wound healing. *Life Sci*. 2024,357:123066.
- [11] Raghav PK, Mann Z. Nano-Delivery Revolution: Harnessing Mesenchymal Stem Cell-Derived Exosomes' Potential for Wound Healing. *Biomedicines*. 2024;12(12):2791.
- [12] Tkach M, Thery C. Communication by extracellular vesicles: where we are and where we need to go. *Cell*. 2016,164 (6): 1226-32.
- [13] Zhang L, Zeng M, Tang F, et al. Circ-PNPT1 contributes to gestational diabetes mellitus (GDM) by regulating the function of trophoblast cells through miR-889-3p/PAK1 axis. *Diabetol Metab Syndr*. 2021,13(1):58.
- [14] Lu GD, Cheng P, Liu T, et al. BMSC-derived exosomal miR-29a promotes angiogenesis and osteogenesis. *Front Cell Dev Biol*. 2020,8:608521.
- [15] Pomatto M, Gai C, Negro F, et al. Differential therapeutic effect of extracellular vesicles derived by bone marrow and adipose mesenchymal stem cells on wound healing of diabetic ulcers and correlation to their cargoes. *Int J Mol Sci*. 2021, 22 (8): 3851.
- [16] Wang C, Wang M, Xu T, et al. Engineering bioactive self-healing antibacterial exosomes hydrogel for promoting chronic diabetic wound healing and complete skin regeneration. *Theranostics*. 2019,9(1):65-76.
- [17] Cao G, Meng X, Han X, et al. Exosomes derived from circRNA Rtn4-modified BMSCs attenuate TNF-alpha-induced cytotoxicity and apoptosis in murine MC3T3-E1 cells by sponging miR-146a. *Biosci Rep*. 2020,40(5).
- [18] Fu M, Fang L, Xiang X, et al. Microarray analysis of circRNAs sequencing profile in exosomes derived from bone marrow mesenchymal stem cells in postmenopausal osteoporosis patients. *J Clin Lab Anal*. 2022,36(1):e23916.
- [19] Zhou J, Ding Y, Zhang Y, et al. Exosomes from bone marrow-derived mesenchymal stem cells facilitate corneal wound healing via regulating the p44/42 MAPK pathway. *Graefes Arch Clin Exp Ophthalmol*. 2023,261(3):723-34.
- [20] Shen C, Tao C, Zhang A, et al. Exosomal microRNA-93-3p secreted by bone marrow mesenchymal stem cells downregulates apoptotic peptidase activating factor 1 to promote wound healing. *Bioengineered*. 2022,13(1):27-37.
- [21] Hui Z, Wang S, Li J, et al. Compound Tongluo Decoction inhibits endoplasmic reticulum stress-induced ferroptosis and promoted angiogenesis by activating the Sonic hedgehog pathway in cerebral infarction. *J Ethnopharmacol*. 2022,283: 114634.
- [22] Yan J, Feng G, Ma L, et al. Metformin alleviates osteoarthritis in mice by inhibiting chondrocyte ferroptosis and improving subchondral osteosclerosis and angiogenesis. *J Orthop Surg Res*. 2022,17(1):333.